# Journal of Materials Chemistry A

Accepted Manuscript




This is an *Accepted Manuscript*, which has been through the Royal Society of Chemistry peer review process and has been accepted for publication.

*Accepted Manuscripts* are published online shortly after acceptance, before technical editing, formatting and proof reading. Using this free service, authors can make their results available to the community, in citable form, before we publish the edited article. We will replace this *Accepted Manuscript* with the edited and formatted *Advance Article* as soon as it is available.

You can find more information about *Accepted Manuscripts* in the Information for Authors.

Please note that technical editing may introduce minor changes to the text and/or graphics, which may alter content. The journal's standard Terms & Conditions and the Ethical guidelines still apply. In no event shall the Royal Society of Chemistry be held responsible for any errors or omissions in this *Accepted Manuscript* or any consequences arising from the use of any information it contains.



ROYAL SOCIETY OF CHEMISTRY

www.rsc.org/materialsA

Journal Name

ARTICLE

# 'Donor-free' oligo(3-hexylthiophene) dyes for efficient dye-sensitized solar cells

Received 00th January 20xx,
Accepted 00th January 20xx

DOI: 10.1039/x0xx00000x

www.rsc.org/

Yue Hu,[a] Aruna Ivaturi,[a] Miquel Planells,[a] Chiara L. Boldrini[b], Alessio Orbelli Biroli,[b] Neil Robertson*[a]

The common trend in designing dyes for use in DSSCs with iodide-based electrolyte is based on a donor - π spacer - acceptor (D-π-A) architecture. Here, we report two 'donor-free' cyanoacrylic end-functionalized oligo(3-hexylthiophene) dyes (**5T** and **6T**). Despite having no donor group, both dyes show reversible first oxidation process. Both **5T** and **6T** have n-hexyl alkyl chains to retard aggregation at different positions as well as different numbers of thiophene moieties. However, the dyes showed similar absorption properties and redox potentials. The DSSCs based on these dyes give power conversion efficiencies of more than 7%, although a significant difference in the $V_{OC}$ and FF has been observed. Using electrochemical impedance spectroscopy, this is attributed to the presence of more trap states when **6T** attaches to $TiO_2$ and modifies the surface, mainly affecting the fill factor. Overall, these dyes introduce a new and effective design concept for liquid-electrolyte DSSC sensitisers.

## Introduction

Over the last 20 years, dye-sensitised solar cells (DSSCs) have attracted significant interest as low-cost alternatives to conventional photovoltaic technologies. They present a record efficiency (uncertified) of ~13% under standard reporting conditions.[1, 2] Ruthenium complexes have been designed to work as sensitisers with standard $I^-/I_3^-$ liquid redox electrolyte, giving a record certified efficiency of 11.9 ± 0.4 %.[3, 4] However, several challenges limit their development for large scale applications including material costs, difficulty in purification and environmental impact. In solid-state dye-sensitised solar cells (ssDSSC) where the liquid based $I^-/I_3^-$ redox couple is exchanged for a hole conductor, thinner $TiO_2$ films are needed because of mass transport limitations or insufficient pore filling. [5-7] Accordingly, metal-free organic sensitisers with high extinction coefficients have been developed and the overwhelming trend in designing these dyes is based on a donor - π spacer - acceptor (D- π -A) architecture.[8, 9] In such dyes, the donor and the π spacer part contain the HOMO of the dye while the LUMO is distributed on the acceptor part and the anchoring group. Upon excitation, the electrons move from donor to acceptor through the π -bridge. This modular design allows organic dyes to show great diversity and flexibility. Cyanoacrylic acid is a commonly used acceptor which decreases the energy gap between HOMO and LUMO, thus leading to a red shift of the lowest energy absorption maximum.[10] Various donor groups have been investigated, including anthraquinone, boradiazaindacene, carbazole, coumarin, *N,N*-diakylaniline, hemicyanine, heteroanthracene, indoline, merocyanine, tetrahydroquinoline, triarylamine, squaraine, perylene and polymeric species. [11] The electron-donor group is usually bulky in order to reduce the electron recombination between redox electrolyte and the $TiO_2$ surface and to stabilize the oxidized dye. The influence of the donor size in D - π - A dye was studied by Yang et al.[9] A higher voltage was observed and reported when a bulky-indoline moiety was introduced as donor into the IQ4 dye.[12]

However, previous study in our group on ssDSSCs using a 'donor-free' sensitiser, cyanoacrylic end-functionalized oligo(3-hexylthiophene) (**5T**) and 'donor- π-acceptor' sensitiser based on the same structure (**MK-2**) showed that without an electron donor group, a significantly-higher open-circuit voltage ($V_{OC}$) could be achieved while the short-circuit current ($J_{SC}$) remained approximately the same. This resulted in a significantly higher over-all efficiency, comparable with the very best dyes for ssDSSCs. Devices using **5T** as the sensitiser and spiro-OMeTAD as the hole-transport material gave an efficiency of 4.4% whereas the ones using **MK-2** as the sensitiser gave only 2.8%. [13]

To follow up the above work, in the present study we have tested **5T** in liquid-state dye-sensitised solar cells using classic $I^-/I_3^-$ redox couple. Another donor-free dye, **6T**, which has one more thiophene unit than **5T**, as well as a simpler synthetic scheme is also designed, synthesised, characterised and tested. To compare the performance

[a] *School of Chemistry, University of Edinburgh, King's Buildings, Edinburgh, EH9 3FJ, UK.*
[b] *Istituto di Scienze e Tecnologie Molecolari del CNR (CNR-ISTM), SmartMatLab Centre, Via C. Golgi 19, 20133 Milano, Italy.*
Electronic Supplementary Information (ESI) available: [details of any supplementary information available should be included here]. See DOI: 10.1039/x0xx00000x

This journal is © The Royal Society of Chemistry 20xx



Please do not adjust margins

Journal of Materials Chemistry A Accepted Manuscript

of 5T and 6T with the traditional D-π-A dyes, we also fabricated the liquid-state dye-sensitised solar cells based on MK2 dye and using $I^-/I_3^-$ redox couple. The dyes studied in the present work have similar molecular backbone as MK2 - both use cyanoacrylic acid as an acceptor group and four thiophene derivatives as a π-spacer. While MK2 has a terminal carbazole donor group to complete the D-π-A structure, 5T and 6T have additional thiophene to elongate the π-system to achieve a molecular size similar to MK2. The best PCE obtained with **MK2**, **5T, 6T** and **N719** are respectively, 5.05%, 7.64%, 7.07% and 8.89% (under the conditions optimized for **N719)**. Most of the D-π-A dyes exhibiting good efficiencies in liquid-state dye-sensitised solar cells have complicated structures and have low synthetic yield.[11] However, the donor-free dyes reported in the present study can be easily synthesised using cross-coupling and have high synthetic yield, opening a new strategy of designing highly efficient 'donor-free' dyes in the future. DSSCs using **6T** showed significantly higher $V_{OC}$ but lower $J_{SC}$ and FF than those using **5T**. By using electrochemical impedance spectroscopy (EIS), it was found that **6T** leads to more trapping states, which may be attributed to the extra conjugation or different position of alkyl chain of **6T** than **5T**.

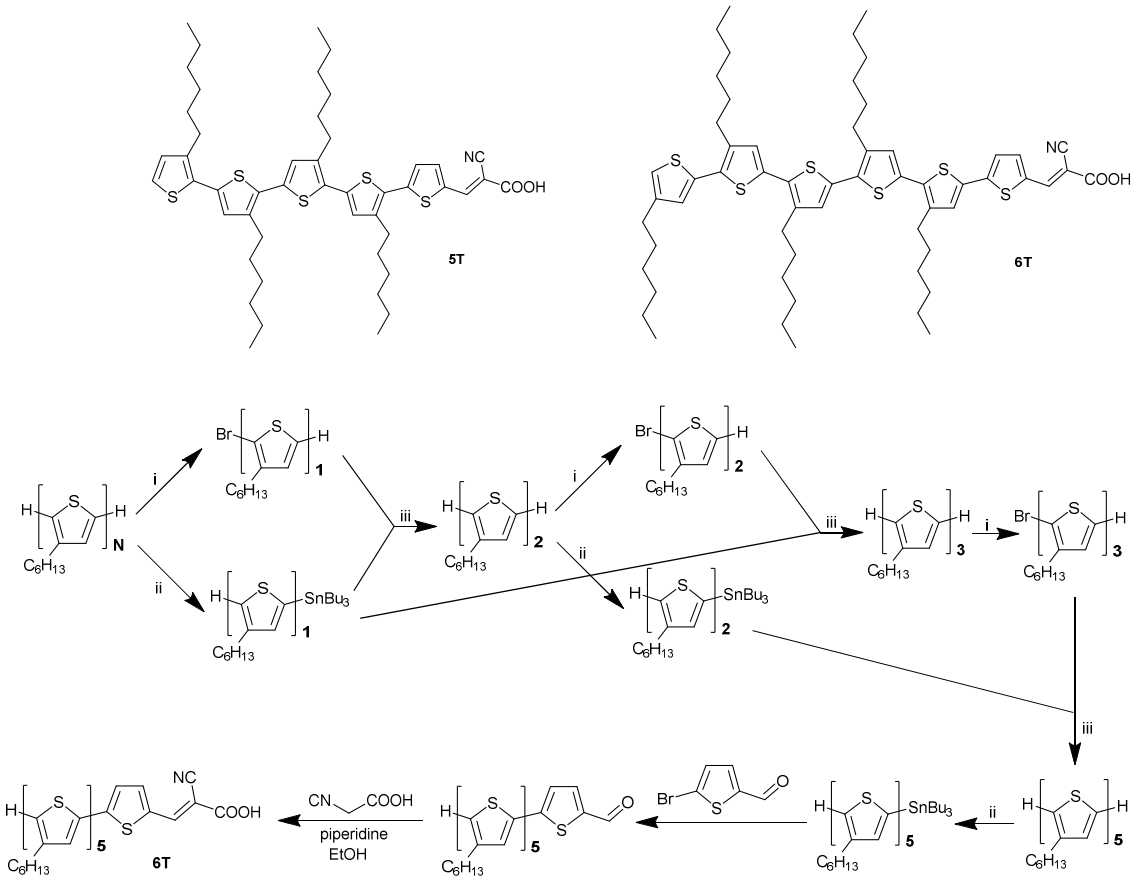


**Scheme 1.** The structure of **5T** and **6T** (above) and the synthetic procedure for the synthesis of **6T**

**Table 1** Photophysical and Electrochemical properties of **5T** and **6T**

| | $\lambda_{max}$ [a] / nm (ε ×$10^{-4}$ / $M^{-1}$ $cm^{-1}$) | $E_{ox}$ [b] vs. NHE/ V | $E_{red}$ [b] vs. NHE / V | $E_{0\text{-}0}$ [c] / eV | $\Delta E_{electrochemical}$ / V | $E^*$ [d] vs. NHE / V |
|---|---|---|---|---|---|---|
| **5T** | 478 (3.9), 376 (2.4) | 1.08 | -1.29 | 2.15 | 2.37 | -1.07 |
| **6T** | 486 (3.9), 401 (3.1) | 0.98 | -1.32 | 2.30 | 2.30 | -1.32 |

[a] Absorption and emission spectra were measured in DCM with a concentration of 2×$10^{-6}$ M at room temperature. [b] Potential was measured in DCM with 0.3 M [TBA][$PF_6$] as electrolyte and calibrated with ferrocene/ferrocenium ($Fc/Fc^+$) as an internal reference and converted to NHE by addition of 0.63 V. [c] 0-0 transition energy, $E_{0\text{-}0}$, estimated from the intercept of the normalized absorption and emission spectra in DCM. [d] Estimated excited state redox potential, estimated by subtracting $E_{0\text{-}0}$ from the ground state oxidation potential.



This journal is © The Royal Society of Chemistry 20xx

Please do not adjust margins

Journal of Materials Chemistry A Accepted Manuscript

Journal Name

ARTICLE

## Results and discussion

### Synthesis

The synthesis of oligo(3-hexylthiophene)s and poly(3-hexylthiophene) has been reported using several routes and the challenge is to separate the high-purity monodisperse regioregular oligo(3-hexylthiophene)s in reasonable quantities. The previous work in our group was based on extending the oligomer stepwise by one unit per cross-coupling followed by activation of the newly formed chain end to give **5T**.[14] This approach was part of a study to prepare shorter oligomers including 1 – 5 thiophene units[14], however it is not very efficient when the longer chains of **5T** and **6T** are specifically desired. In this work, **6T** was therefore synthesised using a 'Fibonacci Route' reported by Heeney. [15] The regioregularity of 6T is proven by the presence (brominated precursor) and absence (stannylated precursor) of 3-bond H-H coupling of the terminal protons in NMR. Also, 6T has a sharp melting point of 132°C. The synthetic route is shown in **Scheme 1**. The synthesis of the oligomer $(3HT)_n$ was achieved by the coupling of Br-$(3HT)_{n-x}$ and $(3HT)_x$-$SnBu_3$. Thus, $(3HT)_n$ with n=1,2,3,5,8,13 and 21 can be obtained more efficiently than adding one thiophene unit per cross-coupling. Also, this strategy allowed easy purification by vacuum distillation of solvent and column chromatography. Finally, in this work, a thiophene unit functionalized with a cyanoacrylic end group was added to enable appropriate attachment to the $TiO_2$. We note that this Fibonacci route leads to alkyl chains in a different position. The alkyl chains for **5T** are at the 3-positions of the thiophene, however, for **6T**, they are at the 2-positions. Alkyl chains were attached to the thiophene unit to avoid strong π- π interaction,[16] which has been proven to lead to a decreased electron injection in the solar cells. [17] Furthemore, alkyl chains play a role in reducing charge recombination between electrons in $TiO_2$ and the redox electrolyte[18].

### Optical Properties

Optical properties of **5T** and **6T** were studied in dichloromethane at $2 \times 10^{-6}$ M. For both dyes, the lowest energy absorption band is around 480 nm. The absorption band positions and their extinction coefficients are summarized in **Table 1**. The addition of thiophene unit and extension of π-system does not lead to significant changes in either the position of the lowest energy absorption band or the extinction coefficient of this band but has a stronger influence on the higher energy band, which corresponds to a π- π* transition of the thiophene backbone and is more intense for **6T**. (**Figure 2**). This assignment was confirmed by measuring UV-vis spectra in different solvents [See the Supporting Information **Figure S2 (a)**]. In a mixture of acetonitrile and butanol, the lowest energy absorption band of both compounds blue shifted significantly while the higher energy band remained at the same wavelength, indicating the charge transfer nature of the lowest energy absorption band. **Figure 2** also gives the absorption spectra of **5T** and **6T** on 3 µm transparent $TiO_2$ films. Both spectra broadened, implying the dyes form Herring-bone aggregates on $TiO_2$ films. [19] **6T** showed wider absorption than **5T** on $TiO_2$ film because of its extra conjugation. This has also been seen by Masumoto, et al.[20], who studied the optical properties of thiophene-based oligomers and found the effective conjugation length of oligothiophenes was six thiophene rings.

Photoluminescence was also studied in solution [see the Supporting Information **Figure S2 (b)**]. **5T** and **6T** both showed very broad emission response, covering the visible and even near-IR region. **5T** showed a bigger Stokes-shift than **6T** (5973 $cm^{-1}$ and 2908 $cm^{-1}$, respectively).

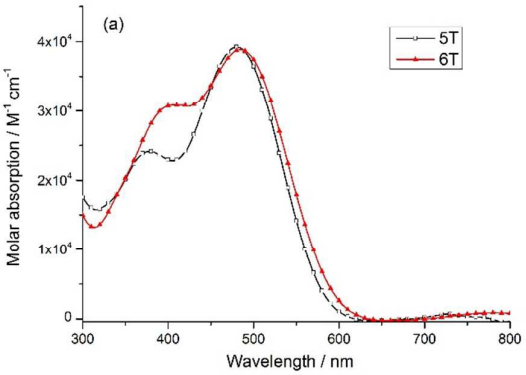


Journal of Materials Chemistry A Accepted Manuscript



Please do not adjust margins

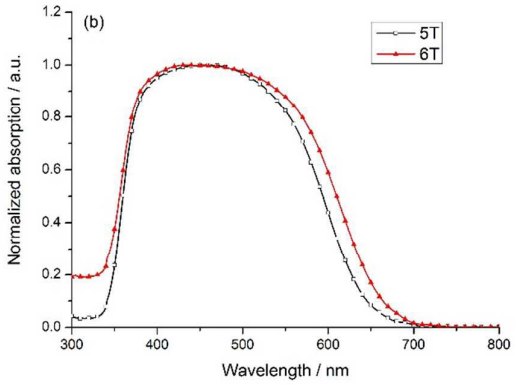


**Figure 2** UV-vis spectra of **5T** and **6T** at $2 \times 10^{-6}$ M in DCM (a) and 3 µm transparent on $TiO_2$ (b)

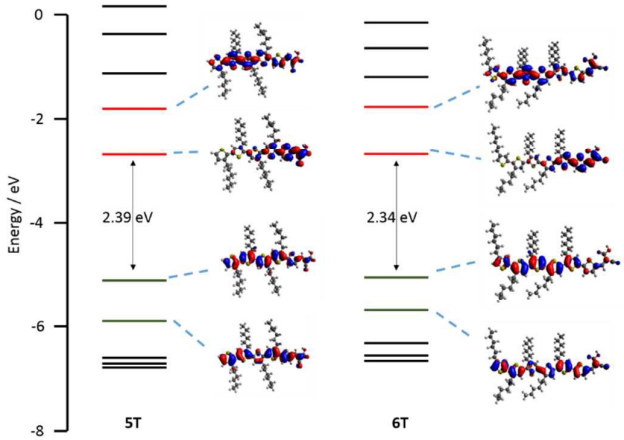


**Figure 3** Energy level schemes for the Kohn-Sham orbitals of **5T** and **6T**, including selected Kohn-Sham orbitals and the HOMO-LUMO energy gap.

**Electrochemical properties and DFT calculations**

Electrochemical properties for **5T** and **6T** were investigated by cyclic voltammetry (CV) and square-wave voltammetry (SWV). Despite the fact that **5T** and **6T** don't have donor groups, both the dyes showed a reversible first oxidation process (Supporting Information, **Figure S3 and S4**). The values against NHE are presented in Table 1. The addition of one more thiophene unit in **6T** shifts the oxidation peak to less positive potential; **5T** shows the first oxidation potential at 1.08V whereas **6T** shows it at 0.98V (see Supporting Information **Table S1-S3**). They are both higher than that of the iodide/triiodide (0.40 V vs. NHE) redox electrolyte energy level, guaranteeing good driving force for the dye regeneration. Little difference was observed for the reduction processes (**5T**: -1.29 V, **6T**: -1.32 V vs. NHE). This is because the LUMO is localized mainly at the cyanoacrylic moiety and is little affected by the length of the thiophene chain. The electrochemical results were supported by DFT calculations. The energy level schemes for the Kohn-Sham orbitals of **5T** and **6T**, including selected Kohn-Sham orbitals and the HOMO-LUMO energy gap are shown in **Figure 3**. For both **5T** and **6T**, the HOMO is distributed along the conjugated π-system and the LUMO is located on the cyanoacetic acid unit through the thiophene, allowing good charge separation and charge directionality after photo-excitation and preventing back regeneration of the dye with the injected electrons. [21] Time-dependent DFT calculation was performed with a dichloromethane polarisable continuum model (PCM)[22] using the CAM-B3LYP functional[23]. The result is consistent with the experimental UV/Vis and is shown in Supporting Information **Table S1-S2**.

**Photovoltaic Performance of DSSCs**

The photovoltaic performance of the DSSCs based on iodide/triiodide redox electrolyte using the **5T** and **6T** dyes was analysed as a function of dye soaking time of 3-24 hours and compared with DSSCs using **N719**. (Supporting information **Figure S4-S6**). The best performance for all the dyes was observed for the devices soaked for 24 hours. To compare the performance of 5T and 6T with the traditional D-π-A dyes, DSSCs based on MK2 dye were also fabricated.The J-V characteristics of the best cells are shown in **Figure 4** and the corresponding device characteristics along with the estimated amount of dye loaded on 18 µm $TiO_2$ photoelectrodes soaked in the corresponding dyes for 24 hours are given in **Table 2**. **N719** has the highest $J_{SC}$ because it exhibits the widest absorption spectrum. The IPCE of DSSCs using **5T** and **6T** (see Supporting Information **Figure S8**) exceeded 60% over most of visible light region from 400 nm to 650 nm, with a maximum of ~80% at around 500 nm and the lowest values were between 650-700 nm. **N719** showed better performance in this region. The slight shift in the absorption onset of the **6T** as compared to **5T** on $TiO_2$ [**Figure 2 (b)**] is also evident from the shift in the IPCE (**Figure S8**) and results in a higher Voc for **6T** compared to **5T (Table 2)**. The absorbed amount of dye increased slightly with increasing the number of thiophene. This can be understood interms of increased π- π interaction with expanding π-conjugation. 6T would form a thicker aggregate on $TiO_2$ surface due to increased number of thiophene and since the adsorbed dye amount of the former is larger than the 5T it would in turn result in slower diffusion of redox species in the mesoporous $TiO_2$ leading to increased charge transfer resistance (as observed in the EIS measurements discussed later) leading to lower FF. A higher dye loading of the **6T** compared to **5T** on $TiO_2$ (**Table 2**), however, doesn't lead to a higher short circuit photocurrent as might be expected. Hagberg et al. observed similar trends in a series of organic chromophores when the π-conjugation between the donor (triphenylamine moiety) and the acceptor (cyanoacetic acid moiety) were systematically extended.[24] A similar trend was also observed by Barea et al. in n-Thiophene absorbers

Journal of Materials Chemistry A Accepted Manuscript



This journal is © The Royal Society of Chemistry 20xx

Please do not adjust margins

when increasing the conjugation length from 2 to 6.[21] Such a decrease in $J_{SC}$ was attributed to the differences in dye binding and orientation affecting injection efficiency.[21,24] Overall, the best PCE efficiencies obtained were **N719** (8.94%), **5T** (7.64%) and **6T** (7.07%). **5T** has a lower PCE than N719 mainly due to a loss in $V_{OC}$, which is not unusual in organic dyes. A significant decrease in the fill factor is observed when comparing the devices using **6T** and others. In contrast, the best PCE efficiency obtained in DSSCs based on **MK2** (processed under conditions optimised for **N719**) is 5.05%, with Jsc of 17.64 mA.cm$^{-2}$, Voc of 0.64 V and FF of 45.0%. The best PCE value reported in literature for MK2 sensitised DSSCs is 8.3% with Jsc of 15.22 mA.cm$^{-2}$, Voc of 0.73 V and FF of 75.0%.[25] The higher Jsc and lower FF observed in the present study could be related to the photoelectrode thickness of 18 µm in contrast to the 16 µm reported in literature. Whereas the lower Voc is related to the electrolyte composition, especially the iodine concentration of 0.2M in the former in contrast to 0.03M used in the present study.

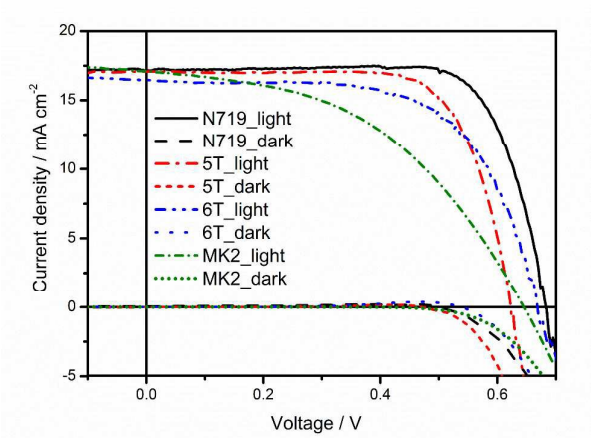


**Figure 4** J-V characteristics and IPCEs of the DSSCs using **N719**, **5T** and **6T** under dark and under AM1.5 simulated sunlight of illumination of 100 mW cm$^{-2}$.

**Table 2** Photovoltaic performance for the champion cells measured under AM 1.5 illumination. The photoelectrodes were soaked in the dye solution for 24 hours.

| Dye | Jsc / mA cm$^{-2}$ | Voc / V | FF / % | Efficiency / % | Dye loading / $\times 10^7$ mol cm$^{-2}$ |
|---|---|---|---|---|---|
| N719 | 17.48 | 0.68 | 74.7 | 8.89 | 3.04 |
| 5T | 17.15 | 0.62 | 72.0 | 7.64 | 5.09 |
| 6T | 16.85 | 0.67 | 62.8 | 7.07 | 5.38 |

**Electrochemical impedance spectroscopy (EIS)**

In order to understand the reasons behind the observed photovoltaic performance as a function of thiophene chain length, detailed impedance spectroscopy measurements were performed on the best cells under illumination from a LED at different bias potentials in the frequencies between 1MHz and 0.1Hz. The data were fitted using the transmission line model. [26, 27] The equivalent circuit is shown in **Figure S9**. From the fittings, charge transfer resistance ($R_{CT}$), electron transport resistance ($R_{trans}$) and chemical capacitance of $TiO_2$ ($C_{Chem}$) were extracted. The electron lifetime and electron transport time were calculated according to the equations: $\tau_e = R_{CT} * C_{Chem}$ and $\tau_{trans} = R_{trans} * C_{Chem}$, respectively. Figure 5 shows the charge transfer resistance and the chemical capacitance of the $TiO_2$ as a function of voltage and the electron lifetime as a function of capacitance. Although it is increasingly common to use the chemical capacitance as a reference for the relative position of the conduction band edge in different devices, Barnes, et al.[28] have highlighted the need to analyse both charge and transport data in addition to simple electron lifetime measurements when drawing conclusions about DSSC behaviour, for the reason that some dyes may modify the distribution of trap states as well as shifting the semiconductor conduction band. Based on this knowledge, we first examine the relationship between transport time and capacitance. The longer transport time of **6T** over **5T** indicates more trap states in the presence of **6T** (**Figure 5 (a)**) also consistent with the higher capacitance for **6T** (**Figure 5 (b)**). A low FF is generally ascribed to high series resistance, [29,30] which includes the redox reaction resistance at the counter electrode, the resistance of electron transport by ions in the electrolyte and electron transport through the $TiO_2$. The longer transport time for **6T** indicates a higher resistance for transport, which leads to a lower FF and a slightly lower $J_{SC}$ for **6T** than the other dyes. This may be caused by the extra conjugation of **6T** compared to **5T**, or the different position of the alkyl chains which modifies the $TiO_2$ surface differently. The longer electron lifetime for **6T** over **5T** [**Figure 5(c)**], despite the higher number of traps, corresponds with the experimental Voc which is higher for **6T**. In contrast, **5T** and **N719** have similar trap states, so any different device behaviour can be attributed to a shift of conduction band edge, possibly related to the different protonation state of **N719** compared with **5T** and **6T**. From **Figure 5 (c) N719** has much longer electron lifetime than **5T** and this leads to a final $V_{OC}$ value trend of **N719**>**6T**>**5T**.

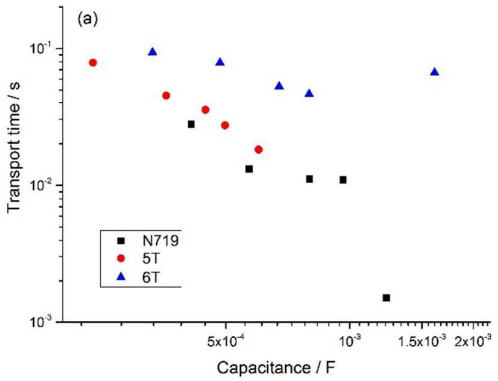


Journal of Materials Chemistry A Accepted Manuscript



Please do not adjust margins

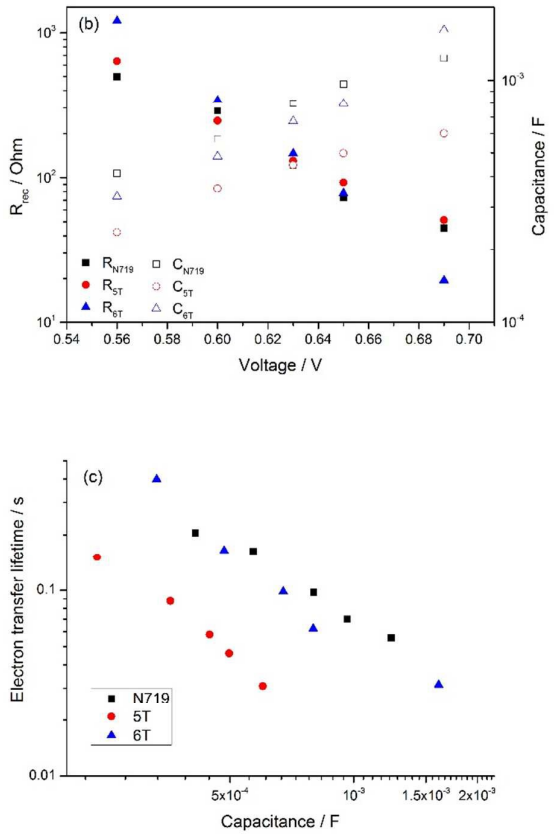


**Figure 5** (a) Transport time plotted against capacitance of the $TiO_2$. (b) Charge transfer resistance and chemical capacitance of the $TiO_2$ plotted against the voltage. (c) Electron lifetime plotted against capacitance of the $TiO_2$.

## Conclusions

Two 'donor-free' cyanoacrylic end-functionalized oligo(3-hexylthiophene) dyes (**5T** and **6T**) have been synthesised, and this dye design used for the first time as effective sensitizers for liquid-state dye-sensitized solar cells with $I^-/I_3^-$ redox couple, giving power conversion efficiency of 7.64% and 7.07%, respectively. **6T** showed a significantly higher $V_{OC}$ than **5T** but lower $J_{SC}$ and FF. By using electrochemical impedance spectroscopy (EIS), it was found that **6T** has more trap states, attributed to the extra conjugation or different position of alkyl chain of **6T**. These dyes can be easily synthesised using cross-coupling and showed reversible first oxidation processes even without donor groups. Overall, this opens up a new strategy for future dye design with the potential for simpler dyes and also new insights into optimised sensitizer design and performance.

## Experimental

### Synthetic procedure

**Materials**. All reagents were purchased from either Sigma-Aldrich or Alfa-Aesar and were used as received without further purification. Tributyl(3,4',4'',4''',4''''-pentahexyl[2,2':5',2'':5'',2''':5''', 2''''-quinquethiophen]-5-yl)-stannane was synthesised according to literature[15] and the detailed experimental method is in the Supporting Information.

Synthesis of **4',4'',4''',4'''',4'''''-pentahexyl-[2,2':5',2'':5'',2''':5''', 2''''':5'''',2''''''-sexithiophen]-5-carbaldehyde** Tributyl(3,4',4'',4''',4''''-pentahexyl[2,2':5',2'':5'',2''':5''',2''''-quinquethiophen]-5-yl)-stannane (800 mg, 0.71 mmol) and 5-bromo-2-thiophenecarboxaldehyde (100 mg, 0.52 mmol) were dissolved in anhydrous toluene (10 ml) and bubbled with $N_2$ for 30 mins. Tetrakis(triphenylphosphine) palladium ($Pd(PPh_3)_4$) (40 mg, 0.035 mmol) was added and the solution was bubbled with $N_2$ for another 10 mins before the solution was heated to 90°C for 72h. The organic solvents were removed by vacuum, then the crude product was purified by column chromatography ($SiO_2$, hexane) to give a red oil (290 mg, 59% yield). $^1$H NMR (500 MHz, $CDCl_3$): 9.48(s, 1H), 7.31(s, 1H), 7.10 (s, 1H), 7.07 (s, 1H), 6.99 (m, 1H), 6.98 (s, 1H), 6.82 (d, J= 4.0Hz, 1H), 6.77 (d, J= 4.0Hz, 1H), 6.60 (m, 1H), 2.87~2.68 (m, 8H), 2.4 (t, J=7.7Hz, 2H), 1.73-1.62 (m, 10H), 1.28-1.15(m, 30H), 0.91-0.84 (m, 15H)

Synthesis of **2-cyano-3-[4',4'',4''',4'''',4'''''-pentahexyl[2,2':5',2'':5'', 2''':5''',2''''':5'''',2''''''-sexithiophen]-5-yl]acrylic acid (6T)** 4',4'',4''', 4'''',4'''''-pentahexyl-[2,2':5',2'':5'',2''':5''',2''''':5'''',2''''''-sexithiophen] -5-carbaldehyde (290 mg, 0.31 mmol) and cyanoacetic acid (40 mg, 0.46 mmol) were dried under vacuum. Then ethanol (2.5 ml) was added and the solution was bubbled with $N_2$ for 10 mins. Piperidine (132 mg, 1.55 mmol) was added and the reaction was heated up to 75°C for 6 h. Then, the mixture was poured into 100 ml of aqueous HCl 1M and extracted with diethyl ether. The crude was purified by size exclusion column chromatography (Biobeads S-X3, DCM) to give a red solid (210 mg, 67% yield). $^1$H NMR (500 MHz, $CDCl_3$): 8.32(s, 1H), 7.70(d, J= 4.2Hz, 1H), 7.29 (s, 1H), 7.25(d, J= 4.0Hz, 1H), 7.04 (s, 1H), 7.01-6.99(m, 2H), 6.98(s, 1H), 6.93(s, 1H), 2.84-2.76(m, 8H), 2.64(t, 7.7Hz, 2H), 1.75-1.64(m, 10H), 1.48-1.32(m, 30H), 0.96-0.90(m, 15H). MS ESI (m/z): $[M]^+$ calcd 1009.41500. Found: 1009.41166. Anal. Calc. for $C_{58}H_{75}NO_2S_6$: C 68.93, H 7.48, N 1.39. Found: C 69.01, H 7.55, N 1.37%. Melting point: 132□.

### Methods

**Chemical characterisation.** $^1$H NMR spectra were recorded on Bruker Advance 500 spectrometer. The deuterated solvents are indicated; chemical shifts, δ, are given in ppm, referenced to TMS, standardized by the solvent residual signal ($^1$H). Coupling constants (J) are given in hertz (Hz). MS were recorded on ThermoElectron MAT 900 using electrospray ionization (ESI) technique. Elemental analyses were carried out by Stephen Boyer at London Metropolitan University using a Carlo Erba CE1108 Elemental Analyser.

**Electrochemical characterisation.** All cyclic voltammetry and square wave voltammetry measurements were carried out in anhydrous

Journal of Materials Chemistry A Accepted Manuscript



This journal is © The Royal Society of Chemistry 20xx

Please do not adjust margins

$CH_2Cl_2$ using 0.3 M [TBA][$PF_6$] electrolyte in a three-electrode system. The solution was purged with $N_2$ prior to measurement. The working electrode was a Pt disk. The reference electrode was Ag/AgCl and the counter electrode was a Pt rod. All measurements were made at room temperature using an μAUTOLAB Type III potentiostat, driven by the electrochemical software GPES. Cyclic voltammetry (CV) measurements used scan rates of 0.1, 0.2, 0.4, 0.6, 0.8 and 1V/s. Square wave voltammetry (SWV) experiments were carried out at a step potential of 4 mV, a square wave amplitude of 25 mV and a square wave frequency of 15 Hz, giving a scan rate of 40 mV/s. Ferrocene was used as internal standard in each measurement and potentials are quoted versus NHE against which ferrocene/ferrocenium was observed at 0.63 V.

**Optical characterisation.** Solution UV-Visible absorption spectra were recorded using Jasco V-670 UV/Vis/NIR spectrophotometer controlled using the SpectraManager software. Photoluminescence (PL) spectra were recorded with Fluoromax-3 fluorimeter controlled by the ISAMain software. All samples were measured in a 1 cm cell at room temp. with dichloromethane as a solvent. Concentration of $2\times10^{-6}$ M were used for UV/Visible and PL.

**Computational details.** The molecular structures were optimised in vacuum, using the software Avogadro[31] to enter the starting geometry. Then the structure was optimised in dichloromethane, using the optimised structure from vacuum. All calculations were carried out using the Gaussian 09 program[32] with the hybrid B3LYP functional[23] and the standard 6-31G(d) basis set. Time-dependent DFT calculations (TD-DFT) were performed using Gaussian 09 program with a dichloromethane polarisable continuum model (PCM)[22] using CAM-B3LYP functional. The 20 lowest singlet electronic transitions were calculated and processed with the GaussSum software package.[33]

**Solar cell fabrication**. To make the working electrodes, fluorine doped tin oxide (FTO) coated glass was washed using 2% Hellmanex solution and then by sonication in distilled water, acetone and methanol. The glasses were further cleaned by UV-ozone cleaner for 20 mins. The cleaned glass was pre-treated with a solution of $TiCl_4$ (40mM in water) at 80 ℃ for 30 mins, rinsed with water and ethanol and sintered at 450 ℃ for 30 mins. The working electrodes were screen printed using commercial $TiO_2$ paste (DSL 18NR-T, Dyesol) as the transparent layer and (DSL 18NR-AO, Dyesol) as the scattering layer. The total thickness of the $TiO_2$ layer was maintained at 18μm and the area of the layer was 0.28 $cm^2$. The films were dried at 125℃ for 6 mins and gradually heated over an hour to 510℃ and annealed for 10 mins using a programmable hotplate. The films were allowed to cool to room temperature and post-treated with $TiCl_4$ (40 mM in water) at 80 ℃ for 30 mins and sintered at 500 ℃ for 30 mins. When the temperature dropped to about 80-100 ℃, the working electrodes were put into 0.5mM dye solution in acetonitrile: t-butanol (1:1) and soaked for different time durations (3-24 hours). The electrodes were removed and washed with the same solvent mixture, to remove any unbound dye molecules. Counter electrodes were prepared by drilling a hole into pre-cut FTO glass. The FTO glass pieces were washed with distilled water, 0.1M HCl in ethanol and finally acetone. The electrodes were heated at 400 ℃ for 15 mins both before and after a layer of Platisol (Solaronix) was applied. The solar cells were then assembled in the sandwich mode where the two electrodes were stuck together using thermoplastic (Surlyn). The electrolyte used was a mixture of 1-butyl-3-methylimidazolium iodide (1.3307 g, 1 M), $I_2$ (0.0381 g, 0.03 M), LiI (0.067 g, 0.1 M), 4-tert butylpyridine (0.3380 g, 0.5 M), guanidine thiocyanate (0.059 g, 0.1 M) in acetonitrile (4.25ml) and valeronitrile (0.75ml). To compare the performance of 5T and 6T with the traditional D-π-A dyes, we also fabricated the DSSCs based on MK2 dye and using the same redox couple mentioned above. The electrolyte was introduced by vacuum suction into the hole and the hole was sealed by cover glass. The J-V measurements were carried out using a computer-controlled digital source meter (Keithley 2400) under simulated AM1.5G irradiation from a solar simulator (92250 A, Newport, USA) under 1 sun equivalent (100 $W/m^2$) condition. A light mask was used on the DSSCs, so the illuminated active area of DSSC was fixed to 0.126 $cm^2$. Incident photon-to-current conversion efficiency (IPCE) measurements were carried out with a Bentham PVE300 photovoltaic spectral response system controlled by BenWin+ software, light intensity was measured by a calibrated silicon photodiode (300-1100 nm).

**Electrochemical impedance spectroscopy (EIS).** Electrochemical impedance spectroscopy (EIS) was performed using the AUTOLAB PGSTAT30 potentiostat controlled by FRA software, version 4.9.007. The cells were measured in a frequency range between 7 MHz and 0.02 Hz with forward bias potentials controlled by the intensity of LED lights. The resulting impedance spectra were analysed with Z-view software (Scribner Associate Inc) version 3.3a on the basis of the two channel transmission line model.

## Acknowledgements

We thank China Scholarship Council, the University of Edinburgh and the EPSRC Apex project (EP/M023532/1) for financial support. Open data: http://dx.doi.org/10.7488/ds/279. C.L.B. and A.O.B. thank Regione Lombardia and Fondazione Cariplo for financial support and the use of instrumentation purchased through the "SmartMatLab Centre" project.

## Notes and references

1. A. Yella, H. W. Lee, H. N. Tsao, C. Y. Yi, A. K. Chandiran, M. K. Nazeeruddin, E. W. G. Diau, C. Y. Yeh, S. M. Zakeeruddin and M. Gratzel, *Science*, 2011, **334**, 629.
2. S. Mathew, A. Yella, P. Gao, R. Humphry-Baker, B. F. E. Curchod, N. Ashari-Astani, I. Tavernelli, U. Rothlisberger, M. K. Nazeeruddin and M. Gratzel, *Nat Chem*, 2014, **6**, 242.
3. M. A. Green, K. Emery, Y. Hishikawa, W. Warta and E. D. Dunlop, *Prog Photovoltaics*, 2015, **23**, 1.
4. R. Komiya, Fukui, A., Murofushi, N., Koide, N., Yamanaka, R., Katayama, H., , presented in part at the Technical Digest, 21st International Photovoltaic Science and Engineering Conference,, Fukuoka, 2011.

Journal of Materials Chemistry A Accepted Manuscript

Please do not adjust margins




5. J. Garcia-Canadas, F. Fabregat-Santiago, H. J. Bolink, E. Palomares, G. Garcia-Belmonte and J. Bisquert, *Synthetic Met*, 2006, **156**, 944.
6. K. Tennakone, G. R. Kumara and A. R. Kumarasinghe, *Semiconductor Science and Technology*, 1995, **10**, 1689.
7. F. Fabregat-Santiago, J. Bisquert, L. Cevey, P. Chen, M. K. Wang, S. M. Zakeeruddin and M. Gratzel, *J Am Chem Soc*, 2009, **131**, 558.
8. E. Gabrielsson, H. Ellis, S. Feldt, H. N. Tian, G. Boschloo, A. Hagfeldt and L. C. Sun, *Adv Energy Mater*, 2013, **3**, 1647.
9. J. B. Yang, P. Ganesan, J. Teuscher, T. Moehl, Y. J. Kim, C. Y. Yi, P. Comte, K. Pei, T. W. Holcombe, M. K. Nazeeruddin, J. L. Hua, S. M. Zakeeruddin, H. Tian and M. Gratzel, *J Am Chem Soc*, 2014, **136**, 5722.
10. Z. S. Wang, Y. Cui, K. Hara, Y. Dan-Oh, C. Kasada and A. Shinpo, *Adv Mater*, 2007, **19**, 1138.
11. A. Hagfeldt, G. Boschloo, L. C. Sun, L. Kloo and H. Pettersson, *Chem Rev*, 2010, **110**, 6595.
12. K. Pei, Y. Z. Wu, A. Islam, Q. Zhang, L. Y. Han, H. Tian and W. H. Zhu, *Acs Appl Mater Inter*, 2013, **5**, 4986.
13. A. Abate, M. Planells, D. J. Hollman, S. D. Stranks, A. Petrozza, A. R. S. Kandada, Y. Vaynzof, S. K. Pathak, N. Robertson and H. J. Snaith, *Adv Energy Mater*, 2014, **4**.
14. M. Planells, A. Abate, H. J. Snaith and N. Robertson, *Acs Appl Mater Inter*, 2014, **6**, 17226.
15. F. P. V. Koch, P. Smith and M. Heeney, *J Am Chem Soc*, 2013, **135**, 13695.
16. M. K. Nazeeruddin, P. Pechy, T. Renouard, S. M. Zakeeruddin, R. Humphry-Baker, P. Comte, P. Liska, L. Cevey, E. Costa, V. Shklover, L. Spiccia, G. B. Deacon, C. A. Bignozzi and M. Gratzel, *J Am Chem Soc*, 2001, **123**, 1613.
17. N. Koumura, Z. S. Wang, S. Mori, M. Miyashita, E. Suzuki and K. Hara, *J Am Chem Soc*, 2006, **128**, 14256.
18. L. Schmidt-Mende, J. E. Kroeze, J. R. Durrant, M. K. Nazeeruddin and M. Gratzel, *Nano Lett*, 2005, **5**, 1315.
19. M. Guo, P. Diao, Y. H. Ren, F. S. Meng, H. Tian and S. M. Cai, *Sol Energ Mat Sol C*, 2005, **88**, 23.
20. Y. Kanemitsu, K. Suzuki, Y. Masumoto, Y. Tomiuchi, Y. Shiraishi and M. Kuroda, *Phys Rev B*, 1994, **50**, 2301.
21. E. M. Barea, R. Caballero, F. Fabregat-Santiago, P. De La Cruz, F. Langa and J. Bisquert, *Chemphyschem*, 2010, **11**, 245.
22. M. Cossi and V. Barone, *Journal of Chemical Physics*, 2001, **115**, 4708.
23. A. D. Becke, *Journal of Chemical Physics*, 1993, **98**, 1372.
24. D. P. Hagberg, J.-H. Yum, H. Lee, F. De Angelis, T. Marinado, K. M. Karls-son, R. Humphry-Baker, L. Sun, A. Hagfeldt, M. Grtzel and M. K. Nazeerud-din, *J. Am. Chem. Soc.* 2008, **130**, 6259.
25. Z-S. Wang, N. Koumura, Y. Cui, M. Takahashi, H. Sekiguchi, A. Mori, T. Kubo, A. Furube and K. Hara, *Chem. Mater.* 2008, **20**, 3993.
26. F. Fabregat-Santiago, J. Bisquert, G. Garcia-Belmonte, G. Boschloo and A. Hagfeldt, *Sol Energ Mat Sol C*, 2005, **87**, 117.
27. F. Fabregat-Santiago, G. Garcia-Belmonte, I. Mora-Sero and J. Bisquert, *Phys Chem Chem Phys*, 2011, **13**, 9083.
28. P. R. F. Barnes, K. Miettunen, X. E. Li, A. Y. Anderson, T. Bessho, M. Gratzel and B. C. O'Regan, *Adv Mater*, 2013, **25**, 1881.
29. J. D. Roy-Mayhew, D. J. Bozym, C. Punckt and I. A. Aksay, *Acs Nano*, 2010, **4**, 6203.
30. F. Fabregat-Santiago, J. Bisquert, E. Palomares, L. Otero, D. B. Kuang, S. M. Zakeeruddin and M. Gratzel, *J Phys Chem C*, 2007, **111**, 6550.
31. M. D. Hanwell, D. E. Curtis, D. C. Lonie, T. Vandermeersch, E. Zurek and G. R. Hutchison, *Journal of Cheminformatics*, 2012, **4**.
32. R. A. Gaussian 09, M. J. Frisch, G. W. Trucks, H. B. Schlegel, G. E. Scuseria, M. A. Robb, J. R. Cheeseman, G. Scalmani, V. Barone, B. Mennucci, G. A. Petersson, H. Nakatsuji, M. Caricato, X. Li, H. P. Hratchian, A. F. Izmaylov, J. Bloino, G. Zheng, J. L. Sonnenberg, M. Hada, M. Ehara, K. Toyota, R. Fukuda, J. Hasegawa, M. Ishida, T. Nakajima, Y. Honda, O. Kitao, H. Nakai, T. Vreven, J. A. Montgomery, Jr., J. E. Peralta, F. Ogliaro, M. Bearpark, J. J. Heyd, E. Brothers, K. N. Kudin, V. N. Staroverov, R. Kobayashi, J. Normand, K. Raghavachari, A. Rendell, J. C. Burant, S. S. Iyengar, J. Tomasi, M. Cossi, N. Rega, J. M. Millam, M. Klene, J. E. Knox, J. B. Cross, V. Bakken, C. Adamo, J. Jaramillo, R. Gomperts, R. E. Stratmann, O. Yazyev, A. J. Austin, R. Cammi, C. Pomelli, J. W. Ochterski, R. L. Martin, K. Morokuma, V. G. Zakrzewski, G. A. Voth, P. Salvador, J. J. Dannenberg, S. Dapprich, A. D. Daniels, O. Farkas, J. B. Foresman, J. V. Ortiz, J. Cioslowski, and D. J. Fox, Gaussian, Inc., Wallingford CT, 2009.
33. N. M. O'Boyle, A. L. Tenderholt and K. M. Langner, *Journal of Computational Chemistry*, 2008, **29**, 839.


Journal of Materials Chemistry A Accepted Manuscript



This journal is © The Royal Society of Chemistry 20xx

Please do not adjust margins

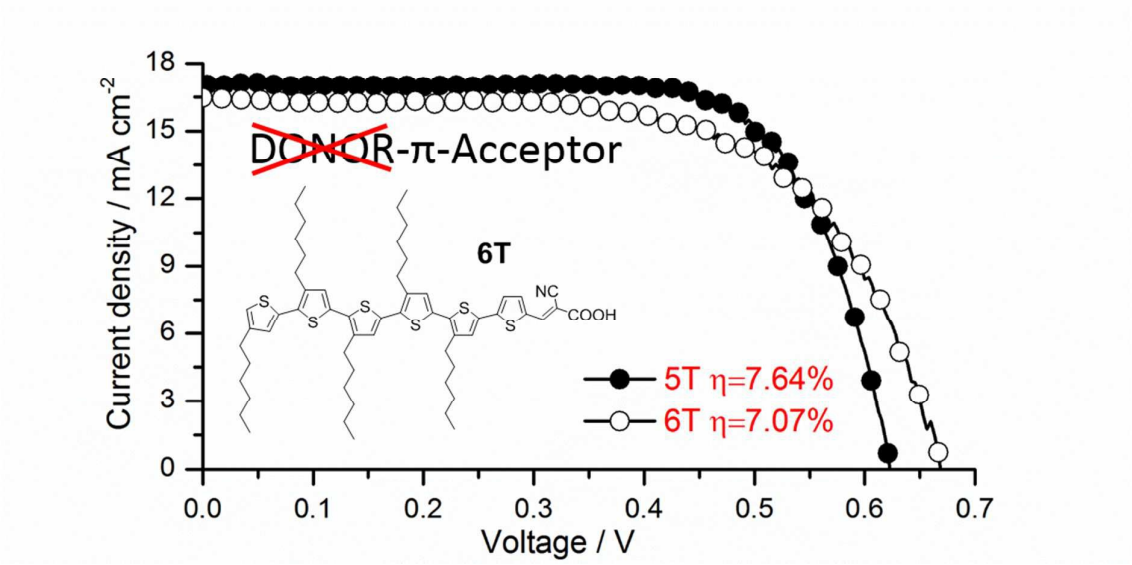


Easily synthesized 'donor-free' dyes work as efficient sensitisers for dye-sensitised solar cells.

Journal of Materials Chemistry A Accepted Manuscript